

RESEARCH

Open Access



# Design, synthesis, biological evaluation, and computational insights of 2-(Aryl)benzo[*d*]imidazo[2,1-*b*]thiazole-7-sulfonamide derivatives as potent antitubercular and antibacterial agents

Hemant S. Deshmukh<sup>1</sup> , Vishnu A. Adole<sup>1\*</sup> , Suraj N. Mali<sup>2</sup> and Bapu S. Jagdale<sup>1\*</sup>

## Abstract

A series of 2-(aryl)benzo[*d*]imidazo[2,1-*b*]thiazole-7-sulfonamide derivatives were synthesized and evaluated for their antitubercular and antibacterial activities, molecular docking, and DFT studies. The compounds were synthesized through a multi-step reactions, with yields varying based on the electronic and steric effects of the substituents. Among the derivatives, **5b**, **5d**, and **5h** exhibited potent antitubercular activity against *Mycobacterium tuberculosis* (H37Rv strain) with minimum inhibitory concentrations (MICs) of 1.6 µg/mL, comparable to some standard drugs like isoniazid. Antibacterial testing revealed that 2-(2,4-dichlorophenyl)benzo[*d*]imidazo[2,1-*b*]thiazole-7-sulfonamide displayed significant activity against Gram-positive bacteria, with MICs as low as 6.25 µg/mL for *Staphylococcus aureus* and *Bacillus subtilis*. The molecular docking and DFT analyses provided insights into the binding interactions and electronic structures of these compounds, with halogen substitutions enhancing biological activity due to increased electron-withdrawing effects. MESP studies showed a distinct electron density distribution, supporting the observed bioactivity. For antitubercular activity, compounds **5b**, **5d**, and **5h** demonstrated potent binding affinities (−6.2 to −5.9 kcal/mol) against the DprE1 enzyme. Compound **5f** showed remarkable antibacterial efficacy, with a docking score of −7.9 kcal/mol against 2,2-dialkylglycine decarboxylase. The DFT analysis revealed that **5a**, with a methoxy substituent, had the highest reactivity (ΔE = 3.86 eV), while halogenated derivatives, such as **5f**, exhibited increased chemical stability (ΔE = 4.24 eV). ADME studies showed that **5f** having favorable lipophilicity and enzyme inhibition. These findings suggested that these derivatives could serve as potential candidates for further drug development against bacterial and mycobacterial infections.

**Keywords** 2-(Aryl)benzo[*d*]imidazo[2,1-*b*]thiazole, Sulphonamides, Antitubercular, Antibacterial, Molecular docking, DFT, Structure–activity relationship

\*Correspondence:

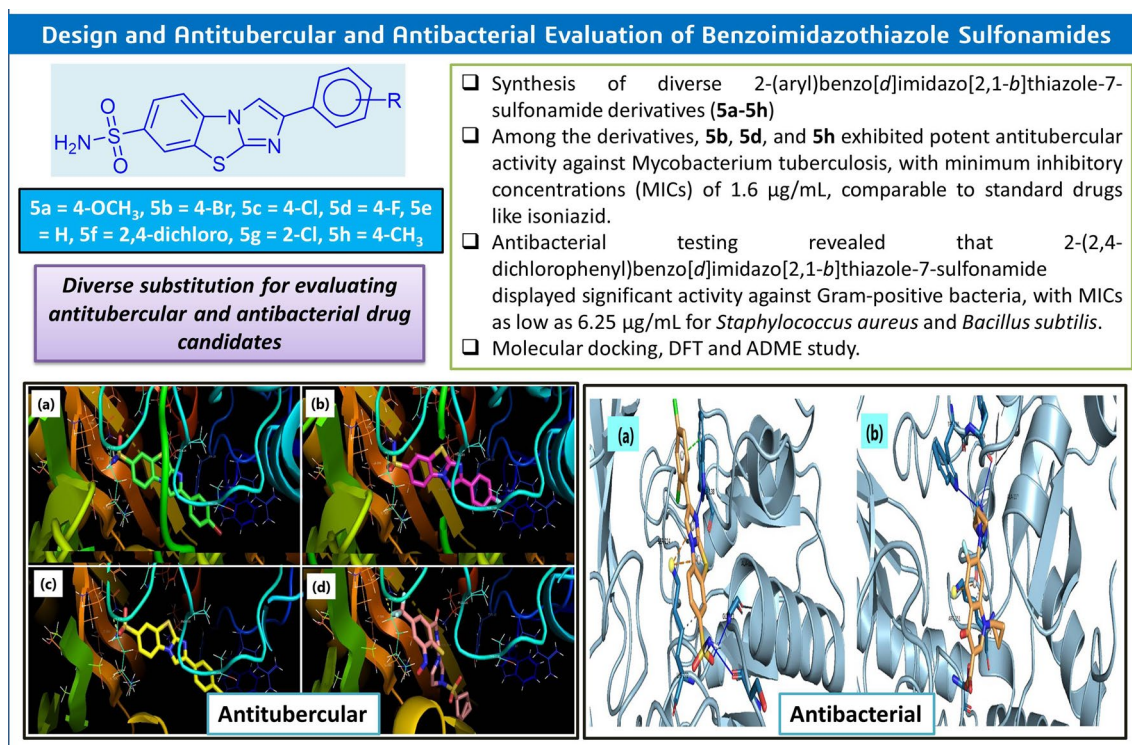
Vishnu A. Adole  
vishnuadole86@gmail.com  
Bapu S. Jagdale  
dr.jagdalebs@gmail.com

Full list of author information is available at the end of the article



© The Author(s) 2025. **Open Access** This article is licensed under a Creative Commons Attribution-NonCommercial-NoDerivatives 4.0 International License, which permits any non-commercial use, sharing, distribution and reproduction in any medium or format, as long as you give appropriate credit to the original author(s) and the source, provide a link to the Creative Commons licence, and indicate if you modified the licensed material. You do not have permission under this licence to share adapted material derived from this article or parts of it. The images or other third party material in this article are included in the article's Creative Commons licence, unless indicated otherwise in a credit line to the material. If material is not included in the article's Creative Commons licence and your intended use is not permitted by statutory regulation or exceeds the permitted use, you will need to obtain permission directly from the copyright holder. To view a copy of this licence, visit <http://creativecommons.org/licenses/by-nc-nd/4.0/>.

## Graphical Abstract



## Introduction

In recent years, benzimidazole and thiazole-based heterocyclic compounds have gained significant attention in the field of medicinal chemistry due to their wide range of biological activities, including antibacterial [1, 2], antitubercular [3, 4], antifungal [5, 6], and anticancer [7, 8] properties. Among these, the imidazo[2,1-*b*]thiazole scaffold has shown promising results in drug discovery for the development of new therapeutic agents [9–13]. The incorporation of sulfonamide functionality within these frameworks is particularly intriguing due to the well-established pharmacophoric nature of sulfonamides, which exhibit potent antimicrobial activities [14, 15]. Given the growing concern over antibiotic resistance and the need for novel therapeutic agents, these chemical structures offer a promising approach to addressing microbial infections, including tuberculosis.

Despite the diverse biological potential of imidazo[2,1-*b*]thiazole derivatives, there remains a gap in exploring their antibacterial and antitubercular properties. Previous studies have largely focused on either the antibacterial or antifungal activities of related compounds, but comprehensive studies that also evaluate their antitubercular efficacy are limited [16–19]. Moreover, while

sulfonamide-containing heterocycles have been widely reported, their synergistic combination with benzimidazo-thiazole scaffolds remains underexplored. Additionally, the incorporation of aryl groups into these systems could further enhance their biological activity, making it necessary to synthesize and evaluate new derivatives with diverse aryl substitutions.

Several studies have reported the antibacterial activities of benzimidazole derivatives. For instance, some analogs have been found to exhibit potent activity against Gram-positive and Gram-negative bacteria by targeting specific bacterial enzymes [20]. Similarly, thiazole-based compounds have demonstrated considerable antibacterial and antitubercular activity through inhibition of bacterial protein synthesis [21]. However, limited studies have comprehensively combined the benzimidazole and thiazole cores with sulfonamide groups to assess their dual antibacterial and antitubercular potential, leaving a gap in the current literature. Figure 1 highlights the some bioactive compounds containing benzothiazole and imidazole structures.

The advent of computational techniques such as molecular docking and density functional theory (DFT) has revolutionized the field of drug discovery [22–24].

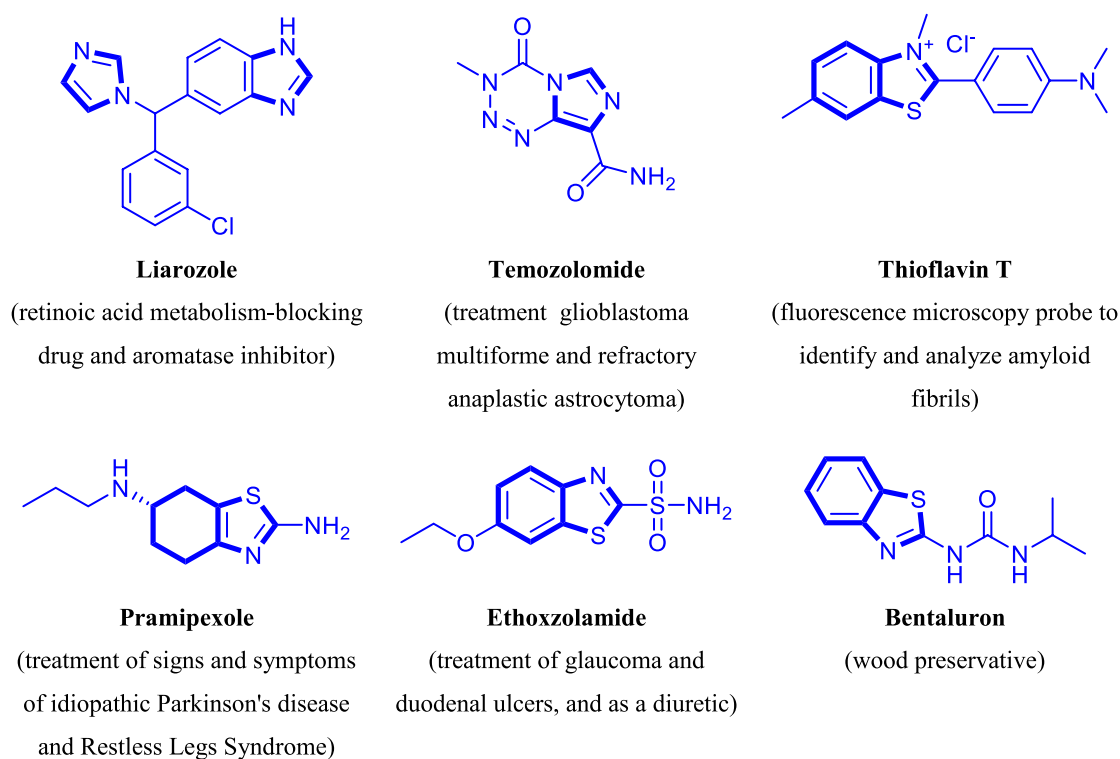


**Fig. 1** Some bioactive compounds containing benzothiazole and imidazole structures

These methods provide insights into the interaction mechanisms between bioactive compounds and their target biomolecules, facilitating the rational design of new therapeutic agents. Molecular docking studies allow researchers to predict the binding affinity and orientation of compounds within the active sites of target proteins, while DFT analysis offers detailed electronic structure information, enabling a deeper understanding of the compounds' reactivity and stability [25–28].

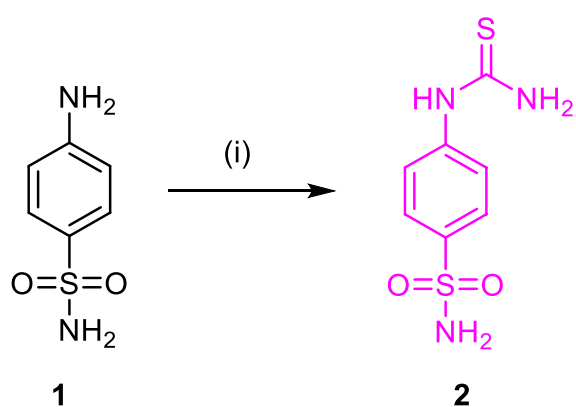
This study is crucial because the rapid emergence of drug-resistant bacterial strains, especially *Mycobacterium tuberculosis*, necessitates the development of new drugs with novel mechanisms of action. The World Health Organization (WHO) has emphasized the urgent need for new antitubercular agents [29]. By investigating the potential of 2-(aryl)benzo[d]imidazo[2,1-b]thiazole-7-sulfonamide derivatives, this research addresses a critical need for novel antimicrobial agents that target both bacterial and tubercular infections. In this work, we aim to synthesize a series of novel 2-(aryl)benzo[d]imidazo[2,1-b]thiazole-7-sulfonamide derivatives and evaluate their antibacterial and antitubercular activities. Furthermore, molecular docking studies are conducted to assess the potential interactions of these compounds with key bacterial and tubercular enzymes. Targeting important enzymes involved in the formation of the

mycobacterial cell wall offers a promising approach in the continuous hunt for new antitubercular and antibacterial medicines. One such target is the enzyme Decaprenylphosphoryl- $\beta$ -D-ribose oxidase (DprE1), which is essential for the production of components of mycobacterial cell walls. DprE1 was chosen as the study's target because to its crucial function in cell wall production and its proven druggability, which is evidenced by the discovery of strong inhibitors that specifically target this enzyme. DFT analysis is performed to explore the electronic properties of the synthesized compounds. This multifaceted approach will provide valuable insights into the structure–activity relationships (SAR) of these derivatives and guide the development of new therapeutic agents.

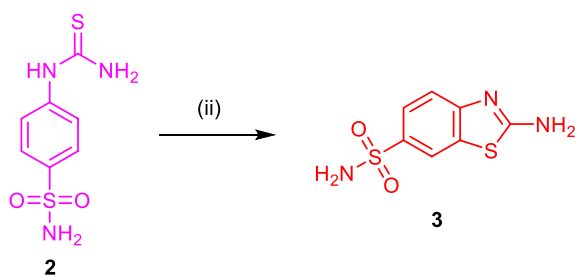
## Materials and methods

### Chemicals and instrumentations

The chemicals (Make: Merck, Sigma Aldrich, and Avra synthesis) with high purity were purchased from Virion Enterprises, Mumbai. The chemicals were used as received without any further purification. Melting points were determined in open capillary and uncorrected. NMR spectra were recorded with a Bruker using DMSO- $d_6$  as the solvent, FT-IR spectra were obtained with potassium bromide pellets. Reactions were monitored by



**Scheme 1** Synthesis of 4-thioureidobenzenesulfonamide. Reaction conditions: (i) Concentrated HCl (3.5 mL), water (30 mL), Ammonium thiocyanate (0.075 mol), 95–100 °C



**Scheme 2** Synthesis of 2-aminobenzo[d]thiazole-6-sulfonamide. Reaction conditions: (ii) CHCl<sub>3</sub> (13.75 mL), rt, Br<sub>2</sub> (0.0143 mol in 15 mL CHCl<sub>3</sub>), 50–55 °C

thin-layer chromatography using aluminium sheets with silica gel 60 F254 (Merck).

#### Procedure for the synthesis of 4-thioureidobenzenesulfonamide (Scheme 1)

In a round-bottom flask, 4-aminobenzenesulfonamide (1, 3.5 g, 0.0375 mol) was dissolved in water (30 mL). Concentrated hydrochloric acid (3.5 mL) was added dropwise to the mixture, and the resulting solution was heated to 100 °C. Ammonium thiocyanate (5.71 g, 0.075 mol) was then added portion wise while maintaining the reaction

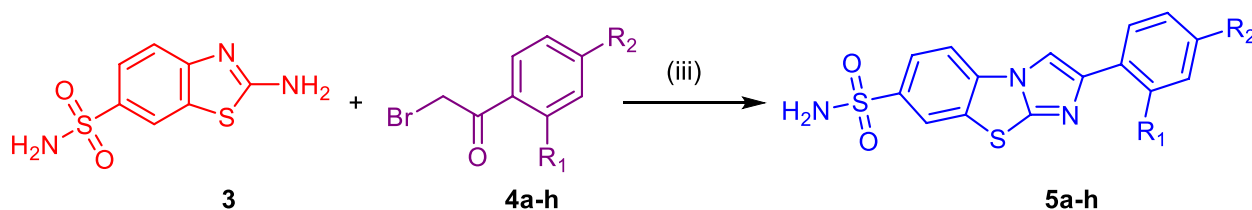
temperature at 95–100 °C. The progress of the reaction was monitored by TLC. Upon completion, the reaction mixture was cooled to 10–15 °C. The precipitated solid was collected by filtration, washed with cold water, and dried to afford the desired product, 2-aminobenzo[d]thiazole-6-sulfonamide (2).

#### Procedure for the synthesis of 2-aminobenzo[d]thiazole-6-sulfonamide (Scheme 2)

A round-bottom flask was charged with 4-thioureidobenzenesulfonamide (2, 2.75 g, 0.01 mol) and chloroform (13.75 mL) at room temperature. Bromine (2.286 g, 0.0143 mol) was diluted in chloroform (15 mL) at room temperature. The bromine solution was then added dropwise to the 4-thioureidobenzenesulfonamide solution while maintaining the temperature at room temperature. During the addition, the temperature of the reaction mixture rose to 40 °C. After the complete addition of the bromine solution, the reaction mixture was stirred at room temperature for 12 h. Subsequently, the reaction mass was heated to 50–55 °C and maintained at this temperature for an additional 12 h. The progress of the reaction was continuously monitored using TLC. Upon completion of the reaction, the solid product was filtered and washed with chloroform. The crude solid was acidified with HCl up to pH 1 and then after filtration the filtrate was basified with ammonia up to pH 12 to offer 2-aminobenzo[d]thiazole-6-sulfonamide (3) as a pure product.

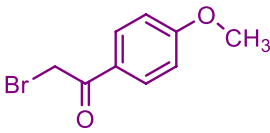
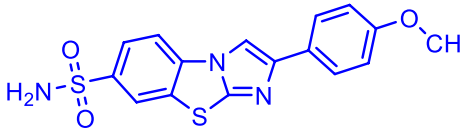
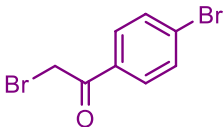
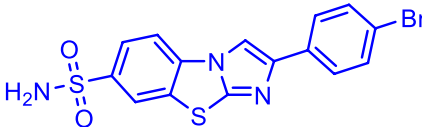
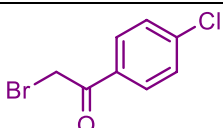
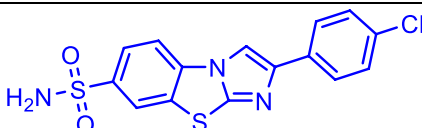
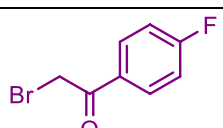
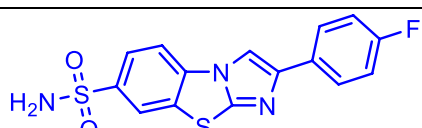
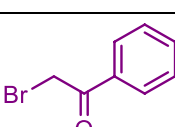
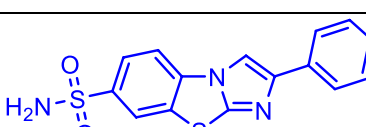
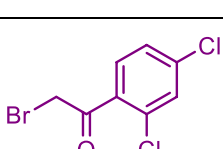
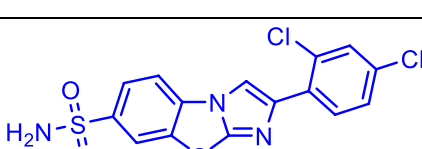
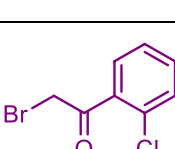
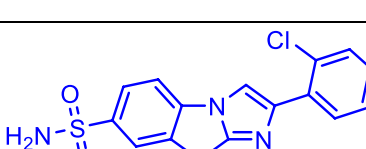
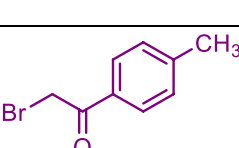
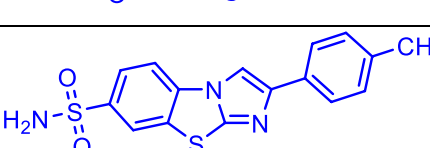
#### Procedure for the synthesis of 2-(aryl)benzo[d]imidazo[2,1-b]thiazole-7-sulfonamide derivatives (Scheme 3)

The starting material, 2-aminobenzo[d]thiazole-6-sulfonamide (3), was reacted with various substituted 2-bromoacetophenones (4a–4h) to yield the corresponding compounds (5a–h). In a typical reaction, 2-aminobenzo[d]thiazole-6-sulfonamide (3, 0.01 mol) was dissolved in a PEG-400 (10 mL) at room temperature. To this solution, the substituted 2-bromoacetophenone derivatives (4a–4h, 0.01 mol) were added for the total eight reactions. The reaction mixture was stirred and heated under reflux for a specific time depending on



**Scheme 3** Synthesis of 2-(aryl)benzo[d]imidazo[2,1-b]thiazole-7-sulfonamide derivatives. Reaction conditions: (iii) PEG-400 (10 mL), reflux

**Table 1** Synthesis of 2-(aryl)benzo[d]imidazo[2,1-b]thiazole-7-sulfonamide derivatives (**5a–5h**)<sup>a</sup>

| Compound  | Phenacyl bromide ( <b>4a–4h</b> )   | Product ( <b>5a–5h</b> )   | Yield <sup>a</sup> (%) | M.P. (°C) |
|-----------|---|--|------------------------|-----------|
| <b>5a</b> |    |    | 89                     | 285–287   |
| <b>5b</b> |    |    | 91                     | 300–302   |
| <b>5c</b> |    |    | 93                     | 312–314   |
| <b>5d</b> |    |    | 90                     | 257–259   |
| <b>5e</b> |   |   | 87                     | 295–297   |
| <b>5f</b> |  |  | 95                     | 305–307   |
| <b>5g</b> |  |  | 93                     | 288–290   |
| <b>5h</b> |  |  | 90                     | 299–301   |

<sup>a</sup> Reaction conditions: all reactant concentrations (0.01 mol), PEG-400 (10 mL), time: 2–3 h; <sup>b</sup> Isolated yields of pure products

the reactivity of the 2-bromoacetophenone derivatives. The progress of the reaction was monitored by thin layer chromatography (TLC). Upon completion, the precipitate was filtered and dried. Then the crude product was purified by recrystallization from methanol solvent to afford the desired products (**5a–5h**) in good to excellent

yields. The resulting compounds (**5a–5h**) were then characterized by spectroscopic techniques, including FT-IR, <sup>1</sup>H NMR, and <sup>13</sup>C NMR to confirm their structure. The physicochemical data is given in Table 1. The spectral images (FT-IR, <sup>1</sup>H NMR, and <sup>13</sup>C NMR) are given in supplementary material.

**Spectral results****2-(4-methoxyphenyl)benzo[d]imidazo[2,1-b]thiazole-7-sulfonamide (5a)**

FT-IR (cm<sup>-1</sup>): 3356, 2959, 1685, 1591, 1545, 1493, 1410, 1247, 1159, 1073, 1022, 897, 819, 738, 700; <sup>1</sup>H NMR (500 MHz, DMSO-*d*<sub>6</sub>) δ 8.70 (s, 1H), 8.55 (d, *J*=1.8 Hz, 1H), 8.12 (d, *J*=8.5 Hz, 1H), 8.01 (dd, *J*=8.5, 1.8 Hz, 1H), 7.81 (d, *J*=8.8 Hz, 2H), 7.50 (s, 2H), 7.02 (d, *J*=8.8 Hz, 2H), 3.80 (s, 3H); <sup>13</sup>C NMR (126 MHz, DMSO-*d*<sub>6</sub>) δ 159.31, 148.24, 147.33, 140.97, 134.23, 130.23, 126.68, 126.61, 124.97, 123.49, 114.71, 113.83, 108.60, 55.62.

**2-(4-bromophenyl)benzo[d]imidazo[2,1-b]thiazole-7-sulfonamide (5b)**

FT-IR (cm<sup>-1</sup>): 3362, 3263, 2982, 1574, 1539, 1495, 1409, 1321, 1207, 1255, 1070, 1004, 953, 879, 811, 692; <sup>1</sup>H NMR (500 MHz, DMSO-*d*<sub>6</sub>) δ 8.89 (s, 1H), 8.57 (d, *J*=1.7 Hz, 1H), 8.13 (d, *J*=8.5 Hz, 1H), 8.02 (dd, *J*=8.5, 1.7 Hz, 1H), 7.83 (d, *J*=8.5 Hz, 2H), 7.64 (d, *J*=8.5 Hz, 2H), 7.52 (s, 2H); <sup>13</sup>C NMR (126 MHz, DMSO-*d*<sub>6</sub>) δ 148.74, 146.09, 141.27, 134.10, 133.30, 132.23, 130.40, 127.21, 125.04, 123.56, 120.84, 114.06, 110.37.

**2-(4-chlorophenyl)benzo[d]imidazo[2,1-b]thiazole-7-sulfonamide (5c)**

FT-IR (cm<sup>-1</sup>): 3337, 3272, 3133, 1575, 1495, 1401, 1324, 1161, 1011, 910, 816, 732, 696; <sup>1</sup>H NMR (500 MHz, DMSO-*d*<sub>6</sub>) δ 8.87 (s, 1H), 8.57 (d, *J*=1.7 Hz, 1H), 8.14 (d, *J*=8.5 Hz, 1H), 8.02 (dd, *J*=8.5, 1.7 Hz, 1H), 7.89 (d, *J*=8.6 Hz, 2H), 7.53–7.50 (m, 4H); <sup>13</sup>C NMR (126 MHz, DMSO-*d*<sub>6</sub>) δ 148.72, 146.06, 141.26, 134.11, 132.94, 132.30, 130.40, 129.32, 126.90, 125.03, 123.56, 114.05, 110.32.

**2-(4-fluorophenyl)benzo[d]imidazo[2,1-b]thiazole-7-sulfonamide (5d)**

FT-IR (cm<sup>-1</sup>): 3588, 3319, 3151, 3036, 1593, 1494, 1412, 1323, 1225, 1159, 1103, 921, 841, 802, 760, 718; <sup>1</sup>H NMR (500 MHz, DMSO-*d*<sub>6</sub>) δ 8.81 (s, 1H), 8.56 (d, *J*=1.7 Hz, 1H), 8.13 (d, *J*=8.5 Hz, 1H), 8.02 (dd, *J*=8.5, 1.7 Hz, 1H), 7.91 (dd, *J*=8.8, 5.5 Hz, 2H), 7.52 (s, 2H), 7.29 (t, *J*=8.9 Hz, 2H); <sup>13</sup>C NMR (126 MHz, DMSO-*d*<sub>6</sub>) δ 162.08 (d, *J*=244.2 Hz), 148.57, 146.35, 141.18, 134.16, 130.61, 130.59, 130.34, 127.20 (d, *J*=8.1 Hz), 125.02, 123.54, 116.19 (d, *J*=21.6 Hz), 113.98, 109.70.

**2-phenylbenzo[d]imidazo[2,1-b]thiazole-7-sulfonamide (5e)**

FT-IR (cm<sup>-1</sup>): 3347, 3152, 3034, 1557, 1500, 1326, 1211, 1152, 1102, 1055, 901, 796, 711; <sup>1</sup>H NMR (500 MHz, DMSO-*d*<sub>6</sub>) δ 8.84 (s, 1H), 8.56 (d, *J*=1.7 Hz, 1H), 8.15 (d, *J*=8.5 Hz, 1H), 8.02 (dd, *J*=8.5, 1.7 Hz, 1H), 7.89 (m, 2H), 7.51 (s, 2H), 7.46 (m, 2H), 7.33–7.30 (m, 1H); <sup>13</sup>C NMR (126 MHz, DMSO-*d*<sub>6</sub>) δ 148.50, 147.28, 141.16, 134.19,

134.03, 130.35, 129.28, 127.98, 125.25, 124.99, 123.53, 114.00, 109.88.

**2-(2,4-dichlorophenyl)benzo[d]imidazo[2,1-b]thiazole-7-sulfonamide (5f)**

FT-IR (cm<sup>-1</sup>): 3492, 3319, 3162, 3094, 1575, 1533, 1497, 1322, 1205, 1155, 1098, 1032, 905, 877, 852, 797, 702; <sup>1</sup>H NMR (500 MHz, DMSO-*d*<sub>6</sub>) δ 9.05–9.02 (m, 1H), 8.57 (d, *J*=1.7 Hz, 1H), 8.40–8.38 (m, 1H), 8.22 (d, *J*=8.6 Hz, 1H), 8.01 (dd, *J*=8.6, 1.8 Hz, 1H), 7.71 (d, *J*=2.2 Hz, 1H), 7.54–7.51 (m, 3H); <sup>13</sup>C NMR (126 MHz, DMSO-*d*<sub>6</sub>) δ 148.19, 142.15, 141.47, 134.21, 132.68, 131.54, 131.12, 131.09, 130.54, 130.20, 128.09, 124.95, 123.48, 114.66, 113.99.

**2-(2-chlorophenyl)benzo[d]imidazo[2,1-b]thiazole-7-sulfonamide (5g)**

FT-IR (cm<sup>-1</sup>): 3319, 3234, 3088, 1595, 1501, 1411, 1320, 899, 785, 695; <sup>1</sup>H NMR (500 MHz, DMSO-*d*<sub>6</sub>) δ 8.62 (d, *J*=1.8 Hz, 1H), 8.56 (d, *J*=8.7 Hz, 1H), 8.04 (dd, *J*=8.7, 1.8 Hz, 1H), 8.01 (t, *J*=1.8 Hz, 1H), 7.99–7.97 (m, 1H), 7.58 (s, 2H), 7.52 (d, *J*=7.8 Hz, 1H), 7.46 (ddd, *J*=8.0, 2.1, 1.0 Hz, 1H); <sup>13</sup>C NMR (126 MHz, DMSO-*d*<sub>6</sub>) δ 149.52, 142.29, 141.65, 134.87, 134.67, 133.81, 131.04, 130.83, 128.29, 126.55, 125.53, 124.73, 123.62, 114.04, 94.14.

**2-(*p*-tolyl)benzo[d]imidazo[2,1-b]thiazole-7-sulfonamide (5h)**

FT-IR (cm<sup>-1</sup>): 3314, 3157, 3011, 1572, 1487, 1409, 1324, 1165, 1104, 931, 914, 816, 718; <sup>1</sup>H NMR (500 MHz, DMSO-*d*<sub>6</sub>) δ 8.60 (d, *J*=1.8 Hz, 1H), 8.56 (d, *J*=8.7 Hz, 1H), 8.03 (dd, *J*=8.7, 1.8 Hz, 1H), 7.89 (d, *J*=8.2 Hz, 2H), 7.55 (s, 2H), 7.31 (d, *J*=8.2 Hz, 2H), 2.36 (s, 3H); <sup>13</sup>C NMR (126 MHz, DMSO-*d*<sub>6</sub>) δ 149.13, 144.16, 141.42, 137.99, 134.78, 130.69, 130.02, 129.63, 127.12, 124.69, 123.59, 113.86, 92.70, 21.35.

**Antitubercular screening**

The antitubercular activity of the synthesized compounds was assessed using the microplate Alamar Blue assay (MABA) against *Mycobacterium tuberculosis* H37Rv strain (ATCC No. 27294). This method, which is non-toxic and employs a thermally stable reagent, provides a good correlation with the proportional and BACTEC radiometric methods. The procedure involved adding 200 μL of sterile deionized water to the outer perimeter wells of a sterile 96-well microplate to minimize evaporation. Subsequently, 100 μL of Middlebrook 7H9 broth was added to the inner wells, and serial dilutions of the test compounds were prepared directly on the plate, with final concentrations ranging from 100 to 0.2 μg/mL. Plates were sealed with parafilm and incubated at 37 °C for 5 days. After this period, 25 μL of a freshly prepared

1:1 mixture of Alamar Blue reagent and 10% Tween 80 were added to each well, followed by 24-h incubation. The results were determined by the color change in the wells: blue indicated no bacterial growth (i.e., effective inhibition by the compound), while pink indicated bacterial growth. The minimum inhibitory concentration (MIC) was defined as the lowest concentration that prevented the color change from blue to pink. Standard antitubercular drugs were used to validate the assay, with MIC values of 1.6  $\mu\text{g}/\text{mL}$  for isoniazid and ethambutol, 3.125  $\mu\text{g}/\text{mL}$  for pyrazinamide, and 0.8  $\mu\text{g}/\text{mL}$  for rifampicin and streptomycin.

#### Antibacterial screening

The serial dilutions of each drug were prepared using brain heart infusion (BHI) broth. Initially, 20  $\mu\text{L}$  of the drug was added to 380  $\mu\text{L}$  of BHI broth in a tube. For the subsequent dilutions, 200  $\mu\text{L}$  of BHI broth was added to each of nine separate tubes. From the initial tube, 200  $\mu\text{L}$  of the drug mixture was transferred to the first tube containing 200  $\mu\text{L}$  of BHI, resulting in a  $10^{-1}$  dilution. This process was repeated sequentially by transferring 200  $\mu\text{L}$  from each preceding tube into the next, up to a  $10^{-9}$  dilution. A 5  $\mu\text{L}$  aliquot of maintained stock cultures of the test organisms was added to 2 mL of BHI broth, and 200  $\mu\text{L}$  of this culture suspension was introduced into each of the serially diluted drug tubes. The tubes were incubated for 24 h and examined for turbidity. For facultative anaerobes, the tubes were incubated at 37  $^{\circ}\text{C}$  for 48–72 h in a  $\text{CO}_2$  jar, while for strict anaerobes, incubation was performed in anaerobic jars for 48–72 h. The BHI broth used was prepared from HIMEDIA M210-500G, containing 200 g/L of calf brain infusion and 250 g/L of beef heart infusion.

#### DFT methodology

All the DFT computations for the synthesized benzothiazoles (**5a–5h**) were performed in gas phase using Gaussian 03 program [30]. The calculations have employed Becke's three parameter hybrid exchange [31] with Lee–Yang–Parr correlation functional (B3LYP) [32] with 6-311G(d,p) basis set. The visualization was done using the Gauss View 4.1.2 molecular visualization program [33].

#### Molecular docking

Protein and ligand preparation, grid generation, and docking were performed using AutoDockTools 1.5.6 [34]. Ligands were optimized in their stable conformation using B3LYP 6-311G(d) with Gaussian 03. 3D crystal structures of proteins were retrieved from the RCSB PDB (IDs: 1D7U, 6G83) based on prior literature [12,

33–37]. Target proteins were pre-processed to remove ligands and water, followed by the addition of Kollman charges and hydrogen bond optimization. Ligands were prepared by adding hydrogen atoms and Gasteiger charges, merging non-polar hydrogens. Docking utilized the Lamarckian Genetic Algorithm, and the best poses were analyzed for ligand-receptor interactions using PyMOL [38]. software (<https://www.pymol.org/>).

#### ADME

The ADME (Absorption, Distribution, Metabolism, and Excretion) study is essential for comprehending a drug's pharmacokinetic profile in the field of drug development. A set of metrics and predictive models helpful in assessing the pharmacokinetics, drug-likeness, and medicinal chemistry friendliness of small compounds can be accessed for free via the web-based program SwissADME [39]. SwissADME, a computational tool developed by the Molecular Modeling Group of the Swiss Institute of Bioinformatics (SIB), uses molecular structure to predict drug-likeness and ADME features. In order to predict these features early in the drug development process, ADME studies make use of sophisticated computer models and in silico tools. This method not only boosts the efficiency of the drug development process but also increases the chances of clinical success by ensuring that only the most promising compounds progress to later testing stages. SwissADME calculates essential metrics such as hydrogen bond donors and acceptors, rotatable bonds, topological polar surface area (TPSA), and solubility. It evaluates lipophilicity using various logP calculations, including iLOGP, XLOGP3, WLOGP, MLOGP, and SILICOS-IT, which are vital for understanding a molecule's capacity to cross cell membranes. Additionally, it predicts the solubility of compounds in water, critical for oral bioavailability. ADME parameters like gastrointestinal absorption, blood–brain barrier penetration, P-glycoprotein substrate status, and interactions with cytochrome P450 enzymes are also predicted, which are crucial for metabolism and potential drug–drug interactions. According to Lipinski's "rule of five," compounds should not have more than 10 hydrogen bond acceptors (HBAs) or 5 hydrogen bond donors (HBDs), and all the compounds' structures should follow these guidelines. Additionally, the topological polar surface area (tPSA), which evaluates the impact of polar fragments on the surface of a molecule, should be no greater than 140  $\text{\AA}^2$ . A higher tPSA may hinder the compound's ability to cross the blood–brain barrier and decrease its membrane permeability.

## Results and discussion

### Chemistry

The synthesis of 2-aminobenzo[*d*]thiazole-6-sulfonamide (**2**) was achieved through a multi-step process starting with the reaction of 4-aminobenzenesulfonamide (**1**) with ammonium thiocyanate under acidic conditions, conducted in water at 95–100 °C. This reaction facilitated the formation of the thiazole ring, confirmed by the precipitation of the product upon cooling. The isolated product was further brominated by adding bromine in chloroform. The reaction was carefully controlled, with the temperature rising to 40 °C during bromine addition, followed by a 24-h reflux at 50–55 °C to ensure complete transformation yielding 2-aminobenzo[*d*]thiazole-6-sulfonamide (**3**). The final step involved reacting compound **3** with various substituted 2-bromoacetophenones (**4a–4h**) in PEG-400, an environmentally friendly solvent. The yields of the final products (**5a–5h**) varied depending on the electronic and steric effects of the substituents on the acetophenone derivatives. The synthesized compounds were characterized using FT-IR, <sup>1</sup>H NMR, and <sup>13</sup>C NMR spectroscopy, confirming their structures and purity. The synthetic route was efficient and reproducible, highlighting the potential of PEG-400 as a sustainable solvent in heterocyclic chemistry. The 2-aminobenzo[*d*]thiazole-6-sulfonamide derivatives synthesized in this study offer promising prospects for further biological evaluation and potential therapeutic applications.

The FT-IR spectra for the compounds **5a–5h** show distinct peaks corresponding to various functional groups. For **5a**, the broad absorption at 3356 cm<sup>-1</sup> is assigned to the sulfonamide (–SO<sub>2</sub>NH<sub>2</sub>) stretching, while the sharp peaks at 2959 and 1574 cm<sup>-1</sup> are attributed to aromatic C–H and C=N stretches, respectively. Similarly, **5b** displays a sulfonamide stretching at 3362 cm<sup>-1</sup>, with additional C=N and C=C vibrations at 1574 cm<sup>-1</sup> and 1539 cm<sup>-1</sup>, respectively. In **5c**, the peak at 3337 cm<sup>-1</sup> confirms the sulfonamide presence, along with C=N stretches around 1575 cm<sup>-1</sup>. Compound **5d** exhibits a similar sulfonamide peak at 3588 cm<sup>-1</sup>, while **5e** shows a slight shift of this stretch to 3347 cm<sup>-1</sup>. For **5f**, the FT-IR spectrum highlights a sulfonamide stretch at 3492 cm<sup>-1</sup>, and in **5g** and **5h**, characteristic sulfonamide stretches are noted at 3319 cm<sup>-1</sup> and 3314 cm<sup>-1</sup>, respectively, with supporting aromatic C=C stretches around 1409–1595 cm<sup>-1</sup> across all compounds. The <sup>1</sup>H NMR spectra reveal significant insights into the chemical environment of protons in these benzimidazole-thiazole derivatives. In **5a**, the singlet at δ 8.70 corresponds to the proton on the benzimidazole ring, while the doublet at δ 8.55 (*J*=1.8 Hz) indicates the coupling between aromatic protons. The methoxy group's protons resonate as a singlet at δ 3.80, highlighting the electron-donating nature of the methoxy

substituent. In **5b**, the downfield shift of the benzimidazole proton to δ 8.89 reflects the electron-withdrawing effect of the bromine substituent. The coupling constant (*J*=1.7 Hz) between protons at δ 8.57 and δ 8.02 reflects ortho-coupling, while the doublet at δ 7.83 is indicative of the para-substituted bromophenyl group. In **5c**, the similar chemical shifts for the chlorophenyl moiety at δ 7.89 and δ 7.50 suggest a deshielding effect due to chlorine's inductive withdrawing property. The coupling constant (*J*=1.7 Hz) remains similar across these derivatives, indicative of weak ortho-coupling. In **5d**, the fluorine atom causes notable changes in the coupling constants (*J*=8.8, 5.5 Hz), with the aromatic protons displaying splitting due to fluorine's electronegativity. The multiplet at δ 7.29 suggests meta- and para-coupling effects within the fluorophenyl ring. Compound **5e** presents a slightly different profile with the phenyl group, with protons appearing as a multiplet around δ 7.89–7.30, reflecting the overlapping signals of the aromatic protons. In **5f**, the presence of two chlorine atoms in the 2,4-positions leads to a downfield shift for the protons at δ 9.05–9.02, further accentuating the electron-withdrawing nature of these groups. The aromatic proton at δ 7.54 in **5g** is also highly deshielded due to chlorine's inductive effects, similar to **5f**. Lastly, in **5h**, the methyl group at the para position leads to a singlet at δ 2.36, indicative of a shielded environment due to the electron-donating methyl group. The <sup>13</sup>C NMR spectra complement the proton data with further structural confirmation. For **5a**, the methoxy carbon resonates at δ 55.62, confirming its attachment to the aromatic ring, while the benzimidazole carbons resonate between δ 159.31 and δ 108.60. In **5b**, the bromophenyl carbons appear at δ 120.84 and δ 110.37, showing the electron-withdrawing nature of bromine. In **5c**, the chlorophenyl carbons appear at δ 148.72 and δ 132.94, reflecting chlorine's deshielding effect. In **5d**, the signal for the carbon directly attached to fluorine is significantly downfield at δ 162.08 (*J*=244.2 Hz), due to the strong C–F coupling. For **5e**, the phenyl carbons resonate between δ 129.28 and δ 109.88, while in **5f**, the dichlorophenyl carbons shift between δ 148.19 and δ 113.99, showing further deshielding. In **5g**, the signals for the chlorophenyl carbons are consistent with similar patterns of electron withdrawal, while in **5h**, the methyl carbon appears shielded at δ 21.35, reinforcing the electron-donating effects observed in the <sup>1</sup>H NMR spectrum. Overall, the FT-IR, <sup>1</sup>H NMR, and <sup>13</sup>C NMR spectra provide comprehensive structural insights into these benzimidazole-thiazole derivatives, showcasing the effects of various substituents on chemical shifts and coupling patterns.

**Table 2** The antitubercular activity of the 2-(aryl)benzo[d]imidazo[2,1-b]thiazole-7-sulfonamide derivatives (**5a–5h**) against *M. tuberculosis* (H37 RV strain) using microplate Alamar Blue assay

| Compounds    | MIC ( $\mu\text{g/mL}$ ) |
|--------------|--------------------------|
| <b>5a</b>    | 6.25                     |
| <b>5b</b>    | 1.6                      |
| <b>5c</b>    | 6.25                     |
| <b>5d</b>    | 1.6                      |
| <b>5e</b>    | 12.5                     |
| <b>5f</b>    | 3.125                    |
| <b>5g</b>    | 6.25                     |
| <b>5h</b>    | 1.6                      |
| Isoniazid    | 1.6                      |
| Ethambutol   | 1.6                      |
| Pyrazinamide | 3.125                    |
| Rifampicin   | 0.8                      |
| Streptomycin | 0.8                      |

### Antitubercular study

The anti-mycobacterial activity of thiazole derivatives was evaluated against *Mycobacterium tuberculosis* using the Microplate Alamar Blue Assay (MABA). The minimum inhibitory concentrations (MICs) of the tested benzo[d]imidazo[2,1-b]thiazole-7-sulfonamide derivatives ranged from 1.6 to 12.5  $\mu\text{g/mL}$ , revealing significant variation in activity depending on the substituents on the phenyl ring (Table 2). Among the compounds, **5b**, **5d** and **5h** exhibited the most potent inhibition with MIC values of 1.6  $\mu\text{g/mL}$ , equivalent to standard antitubercular drugs such as isoniazid and ethambutol. These halogen-substituted derivatives demonstrated strong potential as anti-mycobacterial agents, likely due to the electron-withdrawing nature of bromine and fluorine, which may enhance their interaction with key bacterial enzymes. The **5h** compound also showed significant activity with an MIC of 1.6  $\mu\text{g/mL}$ , comparable to isoniazid, ethambutol, and pyrazinamide. The presence of a methyl group in the para position may play a role in enhancing the compound's bioactivity by increasing lipophilicity and potentially facilitating better penetration into the bacterial cell. The **5f** derivative displayed moderate activity, with an MIC of 3.125  $\mu\text{g/mL}$ , a value matching pyrazinamide, a commonly used first-line antitubercular drug. The two chlorine atoms likely enhance the electron-withdrawing effects, contributing to moderate inhibitory action. In contrast, compounds such as **5a**, **5c**, **5g**, and **5e** demonstrated weaker activity, with MICs of 6.25–12.5  $\mu\text{g/mL}$ . The methoxy group is an electron-donating substituent, which may reduce the inhibitory effect, while the single chlorine atom, in contrast to the dichloro derivative, exhibited reduced activity, likely due to a weaker

electron-withdrawing effect. The structure–activity relationship (SAR) analysis of these derivatives indicates that halogen substitutions, particularly bromine and fluorine in the para position, significantly enhance antimycobacterial activity, likely through increased electron-withdrawing capacity, which improves the compounds' binding affinity to bacterial targets. Conversely, bulkier or electron-donating groups, such as methoxy, resulted in weaker inhibition. Additionally, the presence of two chlorine atoms, as in the **5f** derivative, contributed to moderate inhibition, while single chlorine substitution reduced activity. These findings suggest that specific structural modifications, such as halogenation, play a critical role in enhancing the antimycobacterial potential of thiazole derivatives. The compounds containing 4-bromo, 4-fluoro, and 4-methyl derivatives, with MIC values of 1.6  $\mu\text{g/mL}$ , exhibit strong potential as lead compounds for future development. These results highlight the importance of chemical modifications in the development of novel antitubercular agents, with halogen-substituted thiazole derivatives offering a promising avenue for further exploration.

### Antibacterial study

The present study focuses on the comparative antibacterial activity of eight benzo[d]imidazo[2,1-b]thiazole-7-sulfonamide derivatives against both Gram-negative (*Escherichia coli*, *Klebsiella pneumoniae*) and Gram-positive (*Staphylococcus aureus*, and *Bacillus subtilis*) bacterial strains (Table 3). Gram-negative bacteria, characterized by a more complex outer membrane and efflux pumps, generally present greater resistance to antibacterial agents. In contrast, Gram-positive bacteria have a simpler cell wall structure that may allow for easier penetration by antibacterial compounds, making them more susceptible to many drugs. Understanding the distinction between Gram-negative and Gram-positive bacteria is crucial, as it helps interpret the structure–activity relationships of the tested compounds. All compounds were tested using the broth dilution method, and ciprofloxacin was employed as a standard for comparison. Ciprofloxacin, a well-known broad-spectrum antibiotic, exhibited the highest potency against all strains with a minimum inhibitory concentration (MIC) of 1.25  $\mu\text{g/mL}$ . Among the benzo[d]imidazo[2,1-b]thiazole-7-sulfonamide derivatives, 2-(2,4-dichlorophenyl)benzo[d]imidazo[2,1-b]thiazole-7-sulfonamide displayed the most significant antibacterial activity, particularly against Gram-positive bacteria, with MIC values as low as 6.25  $\mu\text{g/mL}$  for *Staphylococcus aureus* and *Bacillus subtilis*. The improved activity of this compound suggests that the presence of two chlorine atoms on the

**Table 3** The antibacterial activity of the 2-(aryl)benzo[*d*]imidazo[2,1-*b*]thiazole-7-sulfonamide derivatives (**5a–5h**)

| Compounds            | The antibacterial activity in MIC (µg/mL) |                                  |                              |                                |                               |
|----------------------|---|----------------------------------|------------------------------|--------------------------------|-------------------------------|
|                      | <i>E. coli</i> (ATCC 8739)                | <i>K. pneumoniae</i> (ATCC 4352) | <i>S. aureus</i> (ATCC 6538) | <i>B. subtilis</i> (ATCC 6051) | <i>S. aureus</i> (ATCC 33591) |
| <b>5a</b>            | 25  | 25                               | 12.5                         | 12.5                           | 12.5                          |
| <b>5b</b>            | 25  | 25                               | 25                           | 25                             | 25                            |
| <b>5c</b>            | 25  | 25                               | 25                           | 25                             | 25                            |
| <b>5d</b>            | 25  | 25                               | 25                           | 25                             | 25                            |
| <b>5e</b>            | 25  | 25                               | 12.5                         | 12.5                           | 12.5                          |
| <b>5f</b>            | 12.5                                      | 12.5                             | 6.25                         | 6.25                           | 25                            |
| <b>5g</b>            | 25  | 25                               | 25                           | 25                             | 25                            |
| <b>5h</b>            | 25  | 25                               | 6.25                         | 6.25                           | 12.5                          |
| <b>Ciprofloxacin</b> | 1.25                                      | 1.25                             | 1.25                         | 1.25                           | 1.25                          |

phenyl ring may enhance lipophilicity and contribute to better cell wall penetration and interaction with bacterial enzymes. The electron-withdrawing effect of the halogen substituents likely plays a key role in this heightened activity, as seen in the enhanced efficacy of 2-(2,4-dichlorophenyl)benzo[*d*]imidazo[2,1-*b*]thiazole-7-sulfonamide. For Gram-negative bacteria like *E. coli* and *K. pneumoniae*, most derivatives exhibited moderate activity with MIC values of 25 µg/mL, except for the dichlorophenyl derivative, which showed an improved MIC of 12.5 µg/mL. This suggests that structural modifications to increase the permeability of the compounds could further enhance activity against Gram-negative strains. In contrast, several compounds, including 2-(4-methoxyphenyl)benzo[*d*]imidazo[2,1-*b*]thiazole-7-sulfonamide and 2-phenylbenzo[*d*]imidazo[2,1-*b*]thiazole-7-sulfonamide, exhibited good antibacterial activity against Gram-positive *S. aureus* and *Bacillus subtilis*, with MIC values of 12.5 µg/mL. The introduction of electron-donating groups like methoxy (-OCH<sub>3</sub>) and methyl (-CH<sub>3</sub>) at the phenyl ring slightly enhanced activity against Gram-positive strains, suggesting that these substituents may improve the binding affinity of the compounds to bacterial targets.

Interestingly, despite being structurally similar, compounds with 4-bromo, 4-chloro, and 4-fluorophenyl substitutions exhibited uniform activity across both Gram-positive and Gram-negative strains, with MIC values of 25 µg/mL for all tested bacteria. This uniformity in activity suggests that these halogen substitutions might not be as effective in modulating antibacterial properties compared to dichloro substitution.

The study highlights the importance of understanding the structure–activity relationship (SAR) in designing potent antibacterial agents. It is clear that electron-withdrawing halogens, particularly in the dichloro

configuration, enhance the antibacterial potency of these compounds, while simple halogen or alkyl substitutions exhibit more generalized activity. The antibacterial study identifies 2-(2,4-dichlorophenyl)benzo[*d*]imidazo[2,1-*b*]thiazole-7-sulfonamide as the most promising lead compound, particularly for targeting Gram-positive pathogens. Further structural modifications, especially aimed at enhancing activity against Gram-negative bacteria, may lead to the development of more effective antibacterial agents. However, the study also emphasizes that none of the synthesized derivatives were as potent as ciprofloxacin, indicating the need for further optimization of these benzo[*d*]imidazo[2,1-*b*]thiazole-based scaffolds.

#### Molecular structure and MESP study

The optimized geometries of the benzo[*d*]imidazo[2,1-*b*]thiazole-based compounds (**5a–5h**) given in Table 4 shows a planar benzimidazole-thiazole core, promoting extended  $\pi$ -conjugation across the fused rings, which enhances stability. The sulfonamide group attached at position 1 introduces a slight deviation from planarity due to its tetrahedral geometry around the sulfur atom, while the electron-withdrawing nature of this group pulls electron density away from the core. Conversely, the phenyl group attached at position 12, with its electron-donating methoxy substituent at position 16, aligns closely to the plane of the central structure, allowing efficient conjugation and resonance effects. The Molecular Electrostatic Potential (MESP) diagrams for the benzo[*d*]imidazo[2,1-*b*]thiazole-based compounds (**5a–5h**) given in Table 4 highlights the distribution of electrostatic potential over the molecular surface, with color gradients representing areas of electron density. The red regions around the sulfonamide group, particularly the oxygen atoms, indicate zones of high negative potential,

**Table 4** Optimized molecular structures and Molecular electrostatic surface potential of the 2-(aryl)benzo[d]imidazo[2,1-b]thiazole-7-sulfonamide derivatives (5a-5h)

| Compound | Optimized molecular structure | Molecular electrostatic surface potential |
|----------|-------------------------------|---|
| 5a       |                               |   |
| 5b       |                               |   |
| 5c       |                               |   |
| 5d       |                               |   |
| 5e       |                               |   |
| 5f       |                               |   |
| 5g       |                               |   |
| 5h       |                               |   |

**Table 5** Electronic and global descriptors of the of the 2-(aryl)benzo[d]imidazo[2,1-b]thiazole-7-sulfonamide derivatives (**5a-5h**)

| Compound  | $E_{\text{HOMO}}$ (eV) | $E_{\text{LUMO}}$ (eV) | $\Delta E$ (eV) | $\eta$ (eV) | $\mu$ (eV) | IP   | $\omega$ (eV) | $\chi$ (eV) | A (eV) | $\Delta N_{\text{max}}$ (eV) | S (eV <sup>-1</sup> ) |
|-----------|------------------------|------------------------|-----------------|-------------|------------|------|---------------|-------------|--------|------------------------------|-----------------------|
| <b>5a</b> | -5.75                  | -1.89                  | 3.86            | 1.93        | -3.82      | 5.75 | 3.78          | 3.82        | 1.89   | 1.98                         | 0.52                  |
| <b>5b</b> | -6.20                  | -2.10                  | 4.10            | 2.05        | -4.15      | 6.20 | 4.21          | 4.15        | 2.10   | 2.03                         | 0.49                  |
| <b>5c</b> | -6.21                  | -2.09                  | 4.12            | 2.06        | -4.15      | 6.21 | 4.19          | 4.15        | 2.09   | 2.02                         | 0.49                  |
| <b>5d</b> | -6.18                  | -2.05                  | 4.13            | 2.07        | -4.12      | 6.18 | 4.10          | 4.12        | 2.05   | 1.99                         | 0.48                  |
| <b>5e</b> | -6.12                  | -1.99                  | 4.13            | 2.07        | -4.05      | 6.12 | 3.97          | 4.05        | 1.99   | 1.96                         | 0.48                  |
| <b>5f</b> | -6.36                  | -2.13                  | 4.24            | 2.12        | -4.25      | 6.36 | 4.25          | 4.25        | 2.13   | 2.00                         | 0.47                  |
| <b>5g</b> | -6.29                  | -2.02                  | 4.27            | 2.13        | -4.16      | 6.29 | 4.05          | 4.16        | 2.02   | 1.95                         | 0.47                  |
| <b>5h</b> | -5.98                  | -1.94                  | 4.04            | 2.02        | -3.96      | 5.98 | 3.87          | 3.96        | 1.94   | 1.96                         | 0.49                  |

suggesting strong electron density and potential hydrogen-bond acceptor sites. In contrast, the blue regions near the hydrogen atoms of the sulfonamide group represent areas of positive electrostatic potential, making them suitable for nucleophilic interactions. The relatively neutral green and yellow regions across the aromatic rings, including the benzimidazole and phenyl groups, demonstrate areas of moderate electron density, where electron-withdrawing and electron-donating groups influence the overall electron distribution. This distribution highlights the compound's duality, with electron-rich and electron-poor regions influencing its reactivity, binding affinities, and interactions in potential molecular docking or biochemical environments.

#### Electronic and global descriptors' analysis

The results of the frontier molecular orbital (FMO) analysis and global reactivity descriptors (Table 5) for the benzo[d]imidazo[2,1-b]thiazole-7-sulfonamide derivatives (**5a-5h**) reveal significant insights into their electronic properties. These compounds have shown variations in key parameters such as the HOMO ( $E_{\text{HOMO}}$ ), LUMO ( $E_{\text{LUMO}}$ ) energies, energy gap ( $\Delta E$ ), chemical hardness ( $\eta$ ), electronegativity ( $\chi$ ), and electrophilicity index ( $\omega$ ), all of which are crucial for understanding their reactivity and stability. The electron-donating methoxy group in **5a** leads to a relatively higher  $E_{\text{HOMO}}$  value (-5.75 eV), indicating that this compound is more prone to donating electrons compared to other derivatives. The smaller energy gap ( $\Delta E=3.86$  eV) and higher softness ( $S=0.52$  eV<sup>-1</sup>) suggest that **5a** is more reactive, with higher polarizability and less chemical stability. This reflects the influence of the methoxy group, which enhances electron density and reduces the energy gap, favoring reactivity. In contrast, compounds with halogen substituents like **5b** (bromo), **5c** (chloro), **5d** (fluoro), and **5f** (dichloro) exhibit lower  $E_{\text{HOMO}}$  values, ranging from -6.36 eV (**5f**) to -6.18 eV (**5d**), indicating stronger resistance to electron donation and enhanced stability.

The halogen atoms, particularly the dichloro group in **5f**, lead to the largest energy gap ( $\Delta E=4.24$  eV) and the highest chemical hardness ( $\eta=2.12$  eV), indicating that this compound is less reactive but more chemically stable. The electrophilicity index ( $\omega$ ) for **5f** is also the highest at 4.25 eV, suggesting its stronger electrophilic nature, which is favorable for reactions with nucleophiles. The unsubstituted phenyl derivative **5e** presents an intermediate behavior with an  $E_{\text{HOMO}}$  of -6.12 eV and an energy gap of 4.13 eV. Its properties, such as chemical hardness (2.07 eV) and electrophilicity (3.97 eV), are moderate, showing that **5e** balances between stability and reactivity, lacking the strong polarizing effects of electron-withdrawing or donating groups. Compound **5g**, with a 2-chlorophenyl substituent, has a similar reactivity profile to **5f** but with a slightly smaller energy gap (4.27 eV). Interestingly, **5h**, containing an amethyl group, demonstrates a relatively lower energy gap (4.04 eV), slightly higher softness ( $S=0.49$  eV<sup>-1</sup>), and a higher  $E_{\text{HOMO}}$  (-5.98 eV) compared to the halogenated derivatives, reflecting the mild electron-donating effect of the methyl group. Overall, the introduction of electron-withdrawing groups, such as halogens, increases chemical stability, as evidenced by lower  $E_{\text{HOMO}}$  values and higher energy gaps, while electron-donating groups like methoxy and methyl enhance reactivity by raising  $E_{\text{HOMO}}$  and lowering  $\Delta E$ . This study illustrates the clear impact of substituents on the electronic properties and reactivity of the benzo[d]imidazo[2,1-b]thiazole-7-sulfonamide derivatives, providing insights into their potential applications in chemical and pharmaceutical fields.

#### Molecular docking and ADME study

##### For antitubercular target

The DprE enzyme, specifically Decaprenylphosphoryl- $\beta$ -d-ribose 2'-epimerase (DprE1), plays a crucial role in mycobacterial cell wall synthesis [35]. It catalyzes the conversion of Decaprenylphosphoryl-d-ribose (DPR) to decaprenylphosphoryl-2-ketoribose (DPX), which is

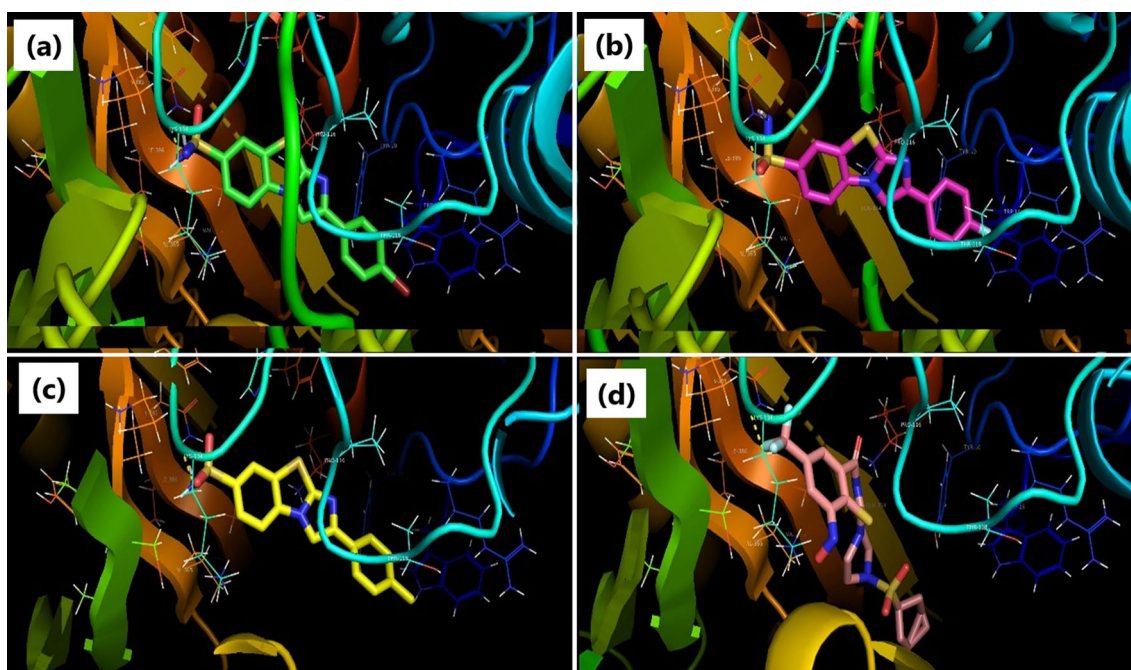


**Fig. 2** Molecular docking interaction diagrams for the best active candidates, **a 5b** [Green], **b 5d** [Pink], **c 5h** [Yellow] and **d EQ8** [Maroon], respectively against the binding site of *Mycobacterium tuberculosis* Decaprenylphosphoryl- $\beta$ -d-Ribose Oxidase (DprE1) enzyme (PDB ID: 6G83)

then further reduced to Decaprenylphosphoryl arabinose [35] (DPA) by DprE2. DPA serves as a key substrate for arabinosyltransferases involved in the synthesis of essential cell wall components, such as arabinogalactan and lipoarabinomannan [35]. Targeting DprE1 offers a promising strategy for developing new anti-TB drugs, especially against drug-resistant strains of *Mycobacterium tuberculosis* [35]. From our in-vitro analysis, we moved forward for molecular docking analysis to check the probable binding modes of the compounds, **5b** [MIC value: 1.6  $\mu\text{g}/\text{mL}$ ], **5d** [MIC value: 1.6  $\mu\text{g}/\text{mL}$ ], and **5h** [MIC value: 1.6  $\mu\text{g}/\text{mL}$ ]. The selection of the pdb id (PDB ID: 6G83, Resolution: 2.40  $\text{\AA}$ , R-Value Work: 0.198) was based on earlier literature report [12] and same was downloaded from protein database bank [<https://www.rcsb.org/structure/6g83>]. The compound **5b** had interactions with amino acid residues such as Lys134, Pro116, Val365, Thr118, Ile386, etc. and obtained as best docked candidate with docking score of  $-6.2$  kcal/mol (Fig. 2). Compounds, **5d** and **5h** showed binding site residues as Lys134, Pro116, Val365, Thr118, Ile386, etc. with binding scores as  $-6.1$  kcal/mol and  $-5.9$  kcal/mol. In all three compounds, we noted the H-bonding interaction with Lys134 amino acid. The co-crystal ligand, EQ8 was also chosen to have comparison of docking affinities and found with score of  $-5.7$  kcal/mol. The EQ8 had interactions with amino acid residues Lys134, Pro116, and Thr118, etc. Our docking validation also resulted the

RMSD value of 1.23  $\text{\AA}$  indicating the correctness of docking protocol followed.

#### For common bacterial target

For antibacterial activity of best in-vitro candidate **5f**, we chosen common antibacterial target as 2,2-dialkylglycine decarboxylase (PDB ID: 1D7U, Resolution: 1.95  $\text{\AA}$ ) [<https://www.rcsb.org/structure/1D7U>] [40]. 2,2-Dialkylglycine decarboxylase (DGD) is an enzyme found in some bacteria that catalyzes the decarboxylation of 2,2-dialkylglycines to produce dialkylamines and carbon dioxide [40]. This reaction is part of bacterial amino acid metabolism, playing a crucial role in the utilization of specific amino acids as nitrogen sources. By facilitating the breakdown of 2,2-dialkylglycines, DGD helps bacteria adapt to diverse environments, enhancing their metabolic flexibility [40]. Additionally, the production of dialkylamines may be involved in various physiological functions, including signalling and osmoregulation. Overall, DGD contributes to bacterial survival and growth under varying conditions [40]. The compound **5f** had best docking score throughout the series as  $-7.9$  kcal/mol, compared to the standard Ciprofloxacin (docking score:  $-6.83$  kcal/mol) (Fig. 3a). Compound **5f** had interactions with amino acid residues such as Ser214, Trp138 (hydrophobic interactions), Gly111 (H-bonding), Lys272 (van der Waals interactions). Standard Ciprofloxacin also retained

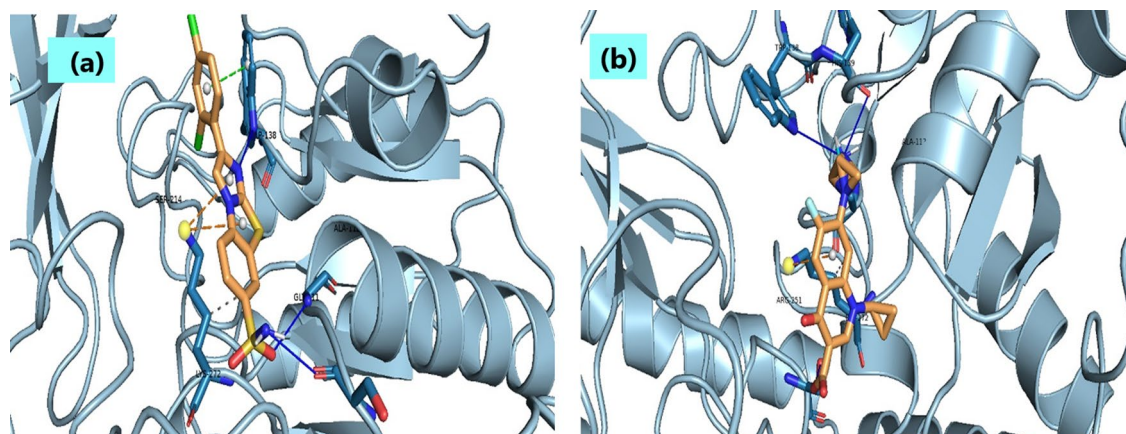


**Fig. 3** Molecular docking interaction diagrams for the best active candidate, **a 5f** and **b Ciprofloxacin**, respectively against the binding site of 2,2-dialkylglycine decarboxylase enzyme (PDB ID: 1D7U)

interactions similar to **5f** with His 139 (H-bonding), Trp138, Ala112, Arg251, Lys272, etc. (Fig. **3b**).

#### ADME study

The ADME and drug-likeness profiles of compounds **5b**, **5d**, **5f**, and **5h** were evaluated, revealing distinct patterns (Table 6). Each compound had 23 to 24 heavy atoms, with no significant variation in the fraction of  $sp^3$  hybridized carbons, except for compound **5h**, which showed a slight increase (0.03). All compounds exhibited two rotatable bonds, suggesting moderate molecular flexibility, while the number of hydrogen bond acceptors varied slightly, with compound **5d** having five and the others four. Each compound possessed one hydrogen bond donor. The molar refractivity values ranged from 86.96 (**5d**) to 97.03 (**5f**), reflecting minor variations in their electronic polarizability. All compounds had the same topological polar surface area (TPSA) of  $114.08 \text{ \AA}^2$ , which indicates that they have comparable polar regions, important for solubility and permeability. The consensus Log Po/w values varied from 2.91 to 3.76, suggesting that compound **5f** is more lipophilic compared to the others. The solubility (Log S, ESOL) values were lowest for **5f** ( $-5.74$ ), indicating poor solubility, while **5d** and **5h** showed relatively better solubility ( $-4.72$  and  $-4.86$ , respectively). Gastro-intestinal (GI) absorption was high for all compounds except **5f**, which exhibited low absorption. None of the compounds permeated the blood–brain barrier (BBB), and they were not substrates for P-glycoprotein (P-gp), indicating limited efflux. All four compounds inhibited CYP1A2, CYP2C19, and CYP2C9 enzymes, but none inhibited CYP2D6. Compound **5h** was the only inhibitor of CYP3A4, indicating potential drug–drug interaction risks for this enzyme. Drug-likeness evaluations

**Table 6** ADME and drug likeness of the compounds **5b**, **5d**, **5f** and **5h**

| ADME parameter        | Compounds              |                        |                        |                        |
|-----------------------|------------------------|------------------------|------------------------|------------------------|
|                       | 5b                     | 5d                     | 5f                     | 5h                     |
| Num. heavy atoms      | 23                     | 23                     | 24                     | 23                     |
| Fraction Csp3         | 00                     | 00                     | 00                     | 0.03                   |
| Num. rotatable bonds  | 2                      | 2                      | 2                      | 2                      |
| Num. H-bond acceptors | 4                      | 5                      | 4                      | 4                      |
| Num. H-bond donors    | 1                      | 1                      | 1                      | 1                      |
| Molar Refractivity    | 94.71                  | 86.96                  | 97.03                  | 91.97                  |
| TPSA                  | $114.08 \text{ \AA}^2$ | $114.08 \text{ \AA}^2$ | $114.08 \text{ \AA}^2$ | $114.08 \text{ \AA}^2$ |
| Consensus Log Po/w    | 3.32                   | 2.91                   | 3.76                   | 2.93                   |
| Log S (ESOL)          | -5.47                  | -4.72                  | -5.74                  | -4.86                  |
| GI absorption         | High                   | High                   | Low                    | High                   |
| BBB permeant          | No                     | No                     | No                     | No                     |
| P-gp substrate        | No                     | No                     | No                     | No                     |
| CYP1A2 inhibitor      | Yes                    | Yes                    | Yes                    | Yes                    |
| CYP2C19 inhibitor     | Yes                    | Yes                    | Yes                    | Yes                    |
| CYP2C9 inhibitor      | Yes                    | Yes                    | Yes                    | Yes                    |
| CYP2D6 inhibitor      | No                     | No                     | No                     | No                     |
| CYP3A4 inhibitor      | No                     | No                     | No                     | Yes                    |
| Lipinski              | Yes                    | Yes                    | Yes                    | Yes                    |
| Ghose                 | Yes                    | Yes                    | Yes                    | Yes                    |
| Veber                 | Yes                    | Yes                    | Yes                    | Yes                    |
| Egan                  | No                     | No                     | Yes                    | Yes                    |
| Muegge                | No                     | No                     | Yes                    | Yes                    |
| Bioavailability Score | 0.55                   | 0.55                   | 0.55                   | 0.55                   |

based on Lipinski, Ghose, and Veber rules were favorable for all compounds, confirming their potential oral bioavailability. However, Egan and Muegge criteria were only met by **5f** and **5h**, which may limit the drug-likeness of **5b** and **5d**. Despite these differences,

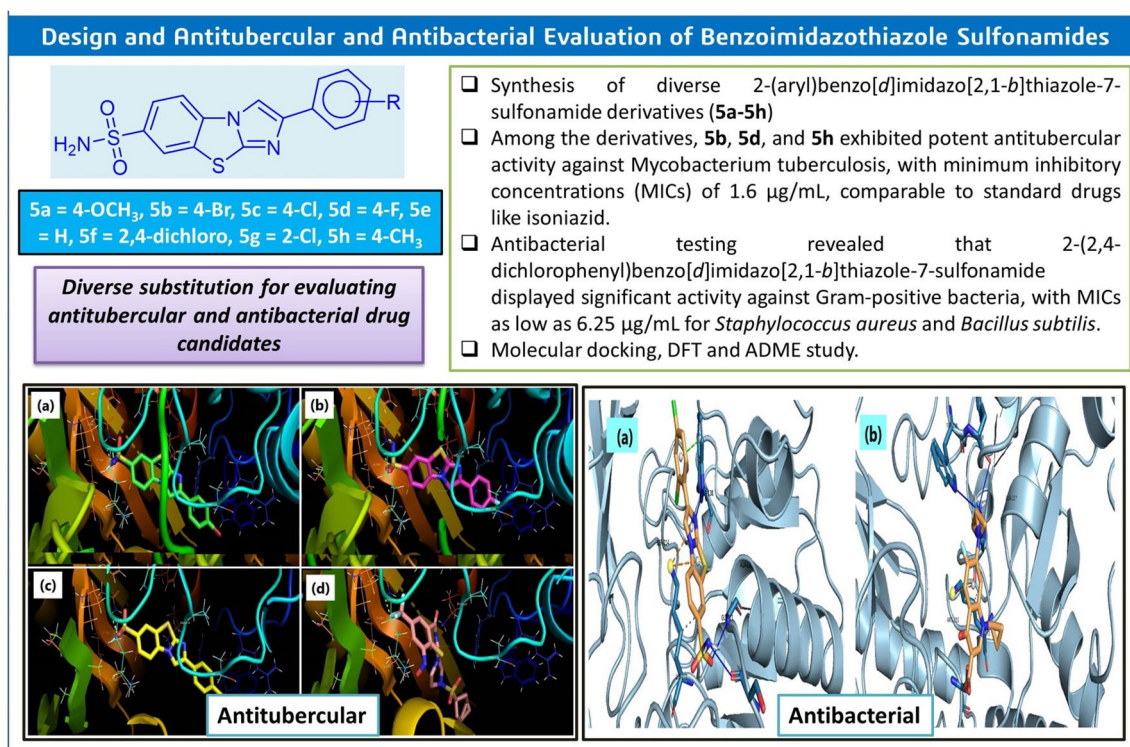


**Fig. 4** Graphical abstract

the bioavailability score was consistent across all compounds (0.55), suggesting moderate bioavailability potential for this series of benzo[d]imidazo[2,1-*b*]thiazole-7-sulfonamide derivatives. The compound **5f** stood out for its higher lipophilicity and distinct enzyme inhibition profile, while **5h** presented slightly improved solubility and drug-likeness.

The graphical abstract, illustrated in Fig. 4, provides a concise and visually engaging summary of the key findings and methodologies of the research work. It serves as a quick reference for readers to understand the core concepts, objectives, and outcomes of the study, highlighting its significance and potential applications in an easily interpretable format.

### Conclusion

The present study highlights the successful synthesis of a series of 2-(aryl)benzo[d]imidazo[2,1-*b*]thiazole-7-sulfonamide derivatives (**5a–5h**), which exhibited significant antibacterial and antitubercular activity. Among the derivatives, compound **5f** showed the highest antibacterial potency with a docking score of  $-7.9$  kcal/mol against 2,2-dialkylglycine decarboxylase, surpassing the standard Ciprofloxacin. Similarly, compounds

**5b**, **5d**, and **5h** exhibited notable antitubercular activity, with binding affinities ranging from  $-6.2$  to  $-5.9$  kcal/mol against the DprE1 enzyme, a critical target in *Mycobacterium tuberculosis*. The DFT analysis provided key insights into the electronic properties of these derivatives, revealing that the presence of electron-donating and withdrawing groups significantly influences their reactivity and stability. Compound **5a**, with a methoxy group, showed the highest reactivity with a lower energy gap ( $\Delta E = 3.86$  eV), while the halogenated derivative **5f** exhibited the highest chemical stability ( $\Delta E = 4.24$  eV), reflecting the impact of substituents on molecular properties. ADME studies revealed that compound **5f** stood out with higher lipophilicity and an optimal enzyme inhibition profile, while compound **5h** showed improved solubility and drug-likeness, making both promising candidates for further drug development. The results from molecular docking, DFT, and ADME analyses underline the potential of these derivatives as antibacterial and antitubercular agents. Future work should focus on optimizing these compounds to enhance their bioavailability and efficacy against drug-resistant pathogens.

## Supplementary Information

The online version contains supplementary material available at <https://doi.org/10.1186/s13065-025-01405-5>.

Supplementary material 1.

### Acknowledgements

The authors acknowledge SAIF, Dharwad, Karnataka for NMR analysis and RAP analytical for FT-IR analysis. Authors also would like to acknowledge Loknete Vyankatrao Hiray Arts, Science and Commerce College Panchavati, Nashik (India) for providing necessary research facilities. The authors also thank School of Pharmacy, D. Y. Patil University, Navi Mumbai, Maharashtra, India for antibacterial screening and Maratha Mandal's NGH Institute of Dental Sciences and Research Centre, Belgaum for antitubercular studies.

### Author contributions

**Hemant Deshmukh:** Conceptualization, Methodology, Software, Data curation, Writing – original draft, Writing – review & editing. **Vishnu A. Adole:** Conceptualization, Supervision, Methodology, Software, Data curation, Writing – original draft, Writing – review & editing. **Bapu S. Jagdale:** Conceptualization, Supervision, Methodology, Software, Data curation, Writing – original draft, Writing – review & editing. **Suraj N. Mali:** Methodology, Software, Data curation, Writing – original draft, Writing – review & editing.

### Funding

No funding was received to carry out the research work.

### Availability of data and materials

All data generated or analyzed during this study are included in this published article [and additionally its supplementary information file includes spectral copies].

### Declarations

#### Ethics approval and consent to participate

Not applicable.

#### Consent for publication

Not applicable.

#### Competing interests

The authors declare no competing interests.

#### Author details

<sup>1</sup>Research Centre in Chemistry, Mahatma Gandhi Vidyamandir's Loknete Vyankatrao Hiray Arts, Science and Commerce College (Affiliated to Savitribai Phule Pune University), Panchavati, Nashik, Maharashtra 422003, India. <sup>2</sup>School of Pharmacy, D. Y. Patil University (Deemed to Be University), Navi Mumbai, Maharashtra 400706, India.

Received: 16 October 2024 Accepted: 30 January 2025

Published online: 14 May 2025

### References

- Zha GF, Preetham HD, Rangappa S, Kumar KSS, Girish YR, Rakesh KP, Ashrafzadeh M, Zarrabi A, Rangappa KS. Benzimidazole analogues as efficient arsenals in war against methicillin-resistance staphylococcus aureus (MRSA) and its SAR studies. *Bioorg Chem.* 2021;115:105175.
- Fouad MM, Farag AM, Elgemeie GH, Shaker NO, Alian NA. Synthesis of novel thiazole-based heterocycles as new antibacterial and antifungal agents. *Egypt J Chem.* 2023;66(13):733–43.
- Parwani D, Bhattacharya S, Rathore A, Mallick C, Asati V, Agarwal S, Rajoriya V, Das R, Kashaw SK. Current insights into the chemistry and antitubercular potential of benzimidazole and imidazole derivatives. *Mini Rev Med Chem.* 2021;21(5):643–57.
- Bhanwala N, Gupta V, Chandrakar L, Khatik GL. Thiazole heterocycle: an incredible and potential scaffold in drug discovery and development of antitubercular agents. *Chem Sel.* 2023;8(46):e202302803.
- Morcos MM, El Shimaa MN, Ibrahim RA, Abdel-Rahman HM, Abdel-Aziz M, Abou El-Ella DA. Design, synthesis, mechanistic studies, and in silico ADME predictions of benzimidazole derivatives as novel antifungal agents. *Bioorg Chem.* 2020;101:103956.
- Kumari G, Dhillon S, Rani P, Chahal M, Aneja DK, King M. Development in the synthesis of bioactive thiazole-based heterocyclic hybrids utilizing phenacyl bromide. *ACS Omega.* 2024;9(17):18709–46.
- Venugopal S, Kaur B, Verma A, Wadhwa P, Magan M, Hudda S, Kakoty V. Recent advances of benzimidazole as anticancer agents. *Chem Biol Drug Des.* 2023;102(2):357–76.
- Shaikh SA, Wakchaure SN, Labhade SR, Kale RR, Alavala RR, Chobe SS, Jain KS, Labhade HS, Bhanushali DD. Synthesis, biological evaluation, and molecular docking of novel 1,3,4-substituted-thiadiazole derivatives as potential anticancer agents. *BMC Chem.* 2024;18(1):119.
- Samala G, Devi PB, Saxena S, Meda N, Yogeeswari P, Sriram D. Design, synthesis, and biological evaluation of imidazo[2,1-b]thiazole and benzo[d]imidazo[2,1-b]thiazole derivatives as Mycobacterium tuberculosis pantothenate synthetase inhibitors. *Bioorg Med Chem.* 2016;24(6):1298–307.
- Karaman B, Ulusoy GN. Synthesis and biological evaluation of new imidazo[2,1-b]thiazole derivatives as anticancer agents. *Med Chem Res.* 2016;25:2471–84.
- Xu WB, Li S, Zheng CJ, Yang YX, Zhang C, Jin CH. Synthesis and evaluation of imidazole derivatives bearing imidazo[2,1-b][1,3,4]thiadiazole moiety as antibacterial agents. *Med Chem.* 2024;20(1):40–51.
- Chirra N, Abburi NP, Rekha EM, Pedapati RK, Bollikanda RK, Murahari M, Sriram D, Sridhar B, Kantevari S. N-substituted piperazine-coupled imidazo[2,1-b]thiazoles as inhibitors of Mycobacterium tuberculosis: Synthesis, evaluation, and docking studies. *Drug Dev Res.* 2024;85(1):e22153.
- Abdel-Maksoud MS, Kim MR, El-Gamal MI, El-Din MMG, Tae J, Choi HS, Lee KT, Yoo KH, Oh CH. Design, synthesis, in vitro antiproliferative evaluation, and kinase inhibitory effects of a new series of imidazo[2,1-b]thiazole derivatives. *Eur J Med Chem.* 2015;95:453–63.
- Ovung A, Bhattacharyya J. Sulfonamide drugs: structure, antibacterial property, toxicity, and biophysical interactions. *Biophys Rev.* 2021;13(2):259–72.
- Mondal S, Malakar S. Synthesis of sulfonamide and their synthetic and therapeutic applications: Recent advances. *Tetrahedron.* 2020;76(48):131662.
- Güzeldemirci NU, Küçükbasmacı Ö. Synthesis and antimicrobial activity evaluation of new 1,2,4-triazoles and 1,3,4-thiadiazoles bearing imidazo[2,1-b]thiazole moiety. *Eur J Med Chem.* 2010;45(1):63–8.
- Dhepe S, Kumar S, Vinayakumar R, Ramareddy SA, Karki SS. Microwave-assisted synthesis and antimicrobial activity of some imidazo[2,1-b][1,3,4]thiadiazole derivatives. *Med Chem Res.* 2012;21:1550–6.
- Morigi R, Vitali B, Prata C, Palomino RA, Graziadio A, Locatelli A, Rambaldi M, Leoni A. Investigation on the effects of antimicrobial imidazo[2,1-b]thiazole derivatives on the genitourinary microflora. *Med Chem.* 2018;14(3):311–9.
- Yang L, Jiao YX, Quan YH, Li MY, Huang XY, Jin JZ, Li S, Quan JS, Jin CH. Synthesis and antimicrobial activity evaluation of pyridine derivatives containing imidazo[2,1-b][1,3,4]thiadiazole moiety. *Chem Biodivers.* 2024;21(4):e202400135.
- Natarajan R, Kumar P, Subramani A, Siraperuman A, Angamuthu P, Bhandare RR, Shaik AB. A critical review on therapeutic potential of benzimidazole derivatives: a privileged scaffold. *Med Chem.* 2024;20(3):311–51.
- Farghaly TA, Alfaihi GH, Gomha SM. Recent literature on the synthesis of thiazole derivatives and their biological activities. *Mini Rev Med Chem.* 2024;24(2):196–251.
- Ram Kumar A, Selvaraj S, Azam M, Sheeja Mol GP, Kanagathara N, Alam M, Jayaprakash P. Spectroscopic, biological, and topological insights on lemnol as a potential anticancer agent. *ACS Omega.* 2023;8(34):31548–66.
- Kumar AR, Selvaraj S, Mol GS, Selvaraj M, Ilavarasan L, Pandey SK, Jayaprakash P, Awasthi S, Albormani O, Ravi A. Synthesis, solvent-solute interactions (polar and non-polar), spectroscopic insights, topological aspects, Fukui functions, molecular docking, ADME, and donor-acceptor investigations of 2-(trifluoromethyl)benzimidazole: a promising candidate for antitumor pharmacotherapy. *J Mol Liq.* 2024;393:123661.

24. Ram Kumar A, Kanagathara N. Spectroscopic, structural, and molecular docking studies on N, N-dimethyl-2-[6-methyl-2-(4-methylphenyl)imidazo[1,2-a]pyridin-3-yl]acetamide. *Phys Chem Res.* 2024;12(1):95–107.
25. Gul S, Jan F, Alam A, Shakoor A, Khan A, AlAsmari AF, Alasmari F, Khan M, Bo L. Synthesis, molecular docking and DFT analysis of novel bis-Schiff base derivatives with thiobarbituric acid for  $\alpha$ -glucosidase inhibition assessment. *Sci Rep.* 2024;14(1):3419.
26. Rochlani S, Bhatia M, Rathod S, Choudhari P, Dhavale R. Exploration of limonoids for their broad-spectrum antiviral potential via DFT, molecular docking and molecular dynamics simulation approach. *Nat Prod Res.* 2024;38(5):891–6.
27. Selvaraj S, Rajkumar P, Kesavan M, Gunasekaran S, Kumaresan S, Rajasekar R, Devi TR. Spectroscopic and quantum chemical investigations on structural isomers of dihydroxybenzene. *J Mol Struct.* 2019;1196:291–305.
28. Thirunavukkarasu K, Rajkumar P, Selvaraj S, Gunasekaran S, Kumaresan S. Electronic structure, vibrational (FT-IR and FT-Raman), UV-Vis and NMR analysis of 5-(4-(2-(5-ethylpyridin-2-yl)ethoxy)benzyl)thiazolidine-2,4-dione by quantum chemical method. *Chem Data Collect.* 2018;17:263–75.
29. Sotgiu G, Sulis G, Matteelli A. Tuberculosis—a World Health Organization perspective. In: Schlossberg D, editor. Tuberculosis and nontuberculous mycobacterial infections. Washington, DC: ASM Press; 2017. p. 211–28.
30. Frish MJ, Trucks GW, Schlegel HB, Scuseria GE, Robb MA, Cheeseman JR, Zakrzewski VG, Montgomery JA Jr, Vreven T, Kudin KN, Burant JC. Gaussian 03, Revision C. 02. Gaussian Inc., 2004; Wallingford, CT.
31. Dennington RD II, Keith T, Millam J. GaussView, Version 4.1.2. Semichem Inc., 2007; Shawnee Mission, KS.
32. Becke AD. Density-functional thermochemistry. III. The role of exact exchange. *J Chem Phys.* 1993;98(7):5648–52. <https://doi.org/10.1063/1.464913>.
33. Lee C, Yang W, Parr RG. Development of the Colle-Salvetti correlation-energy formula into a functional of the electron density. *Phys Rev B.* 1988;37(2):785.
34. Huey R, Morris GM, Forli S. Using AutoDock 4 and AutoDock Vina with AutoDockTools: a tutorial. *Scripps Res Inst Mol Graph Lab.* 2012;10550(92037):1000.
35. Mali SN, Pandey A, Bhandare RR, Shaik AB. Identification of hydantoin-based Decaprenylphosphoryl- $\beta$ -d-Ribose Oxidase (DprE1) inhibitors as antimycobacterial agents using computational tools. *Sci Rep.* 2022;12(1):16368. <https://doi.org/10.2210/pdb4P8C/pdb>.
36. Gurav SS, Waghmode KT, Dandekar SN, Jadhav SD, Lotlikar OA, Jadhav SR, Mali SN, Naphade JG. New 2-Chloroimidazo[1,2-a]pyridine induced Schiff bases: synthesis, characterization, antimicrobial and A-498 and A-549 anticancer activity, molecular modeling, in-silico pharmacokinetics, and DFT studies. *Chem Phys Impact.* 2024;8:100494.
37. Mali SN, Pandey A. Synthesis, computational analysis, antimicrobial, antioxidant, trypan blue exclusion assay,  $\beta$ -hematin assay and anti-inflammatory studies of some hydrazones (part-I). *Curr Comput-Aid Drug Des.* 2023;19(2):108–22.
38. DeLano WL. PyMOL: an open-source molecular graphics tool. *CCP4 Newsl Protein Crystallogr.* 2002;40(1):82–92.
39. Daina A, Michielin O, Zoete V. SwissADME: a free web tool to evaluate pharmacokinetics, drug-likeness and medicinal chemistry friendliness of small molecules. *Sci Rep.* 2017;7(1):42717.
40. Malashkevich VN, Strop P, Keller JW, Jansonius JN, Toney MD. Crystal structures of dialkylglycine decarboxylase inhibitor complexes. *J Mol Biol.* 1999;294(1):193–200.

## Publisher's Note

Springer Nature remains neutral with regard to jurisdictional claims in published maps and institutional affiliations.